

Decadal Trends in the Ocean Carbon Sink

Tim DeVries^{a,b,1}, Corinne Le Quéré^c, Oliver Andrews^{c,d}, Sarah Berthet^e, Judith Hauck^f, Tatiana Ilyina^h, Peter Landschützer^h, Andrew Lenton^{i,j,k}, Ivan D. Lima^l, Michael Nowicki^{a,b}, Jörg Schwinger^m, and Roland Séférian^e

^aDepartment of Geography, University of California, Santa Barbara, CA, USA; ^bEarth Research Institute, University of California, Santa Barbara, CA, USA; ^cTyndall Centre for Climate Change Research, School of Environmental Sciences, University of East Anglia, Norwich, UK; ^dSchool of Geographical Sciences, University of Bristol, Bristol, UK; ^eCentre National de Recherche Météorologique, Unite mixte de recherche, Toulouse, France; ^fAlfred-Wegener-Institut, Helmholtz-Zentrum für Polar und Meeresforschung, Germany; ^hMax Planck Institute for Meteorology, Hamburg, Germany; ⁱCSIRO Oceans and Atmosphere, Hobart, Australia; ^jCentre for Southern Hemisphere Oceans Research, Hobart, Australia; ^kAntarctic Climate and Ecosystems Cooperative Research Centre, Hobart, Australia; ^lDepartment of Marine Chemistry and Geochemistry, Woods Hole Oceanographic Institution, Woods Hole, MA, USA; ^mNORCE Norwegian Research Centre, Bjerknes Centre for Climate Research, Bergen, Norway

This manuscript was compiled on April 8, 2019

1 **Measurements show large decadal variability in the rate of CO₂ ac-**
2 **cumulation in the atmosphere that is not driven by CO₂ emissions.**
3 **The decade of the 1990s experienced enhanced carbon accumula-**
4 **tion in the atmosphere relative to emissions, while in the 2000s the**
5 **atmospheric growth rate slowed even though emissions grew rapidly.**
6 **These variations are driven by natural sources and sinks of CO₂ due**
7 **to the ocean and the terrestrial biosphere. In this study we compare**
8 **three independent methods for estimating oceanic CO₂ uptake, and**
9 **find that the ocean carbon sink could be responsible for up to 40%**
10 **of the observed decadal variability in atmospheric CO₂ accumula-**
11 **tion. Data-based estimates of the ocean carbon sink from pCO₂ map-**
12 **ping methods and decadal ocean inverse models generally agree on**
13 **the magnitude and sign of decadal variability in the ocean CO₂ sink**
14 **at both global and regional scales. Simulations with ocean biogeo-**
15 **chemical models confirm that climate variability drove the observed**
16 **decadal trends in ocean CO₂ uptake, but also demonstrate that the**
17 **sensitivity of ocean CO₂ uptake to climate variability may be too**
18 **weak in models. Furthermore, all estimates point toward coherent**
19 **decadal variability in the oceanic and terrestrial CO₂ sinks, and this**
20 **variability is not well-matched by current global vegetation models.**
21 **Reconciling these differences will help to constrain the sensitivity of**
22 **oceanic and terrestrial CO₂ uptake to climate variability, and lead to**
23 **improved climate projections and decadal climate predictions.**

Carbon dioxide | Ocean carbon sink | Terrestrial carbon sink | Climate variability | Carbon budget

1 **A**nthropogenic emissions of carbon dioxide (CO₂) are a
2 major contributor to climate change, accounting for more
3 than 80% of the radiative forcing of anthropogenic greenhouse
4 gases over the past several decades (1). There is therefore a
5 pressing need to understand the factors influencing the rate at
6 which anthropogenic CO₂ accumulates in the atmosphere. The
7 primary driver of atmospheric CO₂ accumulation is anthro-
8 pogenic emissions from industrial activity and deforestation
9 (2) which has increased by about 60% over the past 30 years
10 (Fig. 1a). CO₂ accumulation in the atmosphere, however,
11 has not always followed the trend in CO₂ emissions. From
12 1990-1999 atmospheric CO₂ accumulated more rapidly than
13 expected from the relatively slow growth in emissions, while
14 in the decade from 2000-2009 atmospheric CO₂ accumulation
15 was relatively steady while emissions rose rapidly (Fig. 1a).

16 This decadal variability in atmospheric CO₂ accumulation
17 rate is linked to variability in the sources and sinks of CO₂
18 in the natural environment (4). The most important of these
19 natural sources and sinks are terrestrial ecosystems and ocean
20 waters. Other natural sources and sinks such as volcanoes
21 and rock weathering are much smaller and change very slowly
22 (5), and can be neglected on recent timescales. Thus, the

global carbon budget (3) is primarily a balance between an-
thropogenic CO₂ emissions from fossil fuel burning and cement
manufacturing (FF) and land-use change (LUC, i.e. defor-
estation), and changes in the accumulation of CO₂ in the
atmosphere (C_{atm}), ocean (C_{oce}) and land biosphere (C_{land}),

$$(FF+LUC) - \frac{dC_{atm}}{dt} - \frac{dC_{oce}}{dt} - \frac{dC_{land}}{dt} = 0. \quad [1]$$

Global FF and LUC emissions have an uncertainty of about
10% (3, 6, 7), and atmospheric CO₂ has been measured con-
tinuously since 1980 at a global network of stations, with error
on the annual average accumulation of < 5% (8). From these
observations and equation (1), we can infer the accumulation
rate of carbon in the combined land and ocean reservoirs
(Fig. 1a). The total rate of land+ocean carbon accumulation
has averaged 55±10% of total carbon emissions over the past
30 years, but has shown significant decadal variability. The
1990s experienced a weakening of the land+ocean carbon sink,
while the first decade of the 2000s was characterized by a
strengthening land+ocean carbon sink (Fig. 1b).

The relative contribution of the land and ocean carbon sinks
to this decadal variability cannot be directly measured, due to
the heterogeneity of carbon accumulation and large natural
carbon reservoirs. For this reason, dynamic global vegetation
models (DGVMs) and global ocean biogeochemistry models
(GOBMs) are often used to estimate the land and ocean carbon
sinks, respectively (3). Methods have also been developed for

Significance Statement

The ocean and land absorb anthropogenic CO₂ from industrial fossil-fuel emissions and land-use changes, helping to buffer climate change. Here we compare decadal variability of ocean CO₂ uptake using three independent methods, and find that the ocean could be responsible for as much as 40% of the observed decadal variability of CO₂ accumulation in the atmosphere. The remaining variability is due to variability in the accumulation of carbon in the terrestrial biosphere. Models capture these variations, but not as strongly as the observations, implying that CO₂ uptake by the land and ocean is more sensitive to climate variability than currently thought. Models must capture this sensitivity in order to provide accurate climate predictions.

TD and CLQ designed the study. TD produced the figures and wrote the manuscript with input from CLQ and PL. OA, SB, JH, TI, AL, IL, JS, RS, and RW performed the global ocean biogeochemistry model simulations and provided input on the manuscript. MN analyzed results from the global ocean biogeochemistry models.

The authors declare no conflict of interest.

¹To whom correspondence should be addressed. E-mail: tdevriesgeog.ucsb.edu

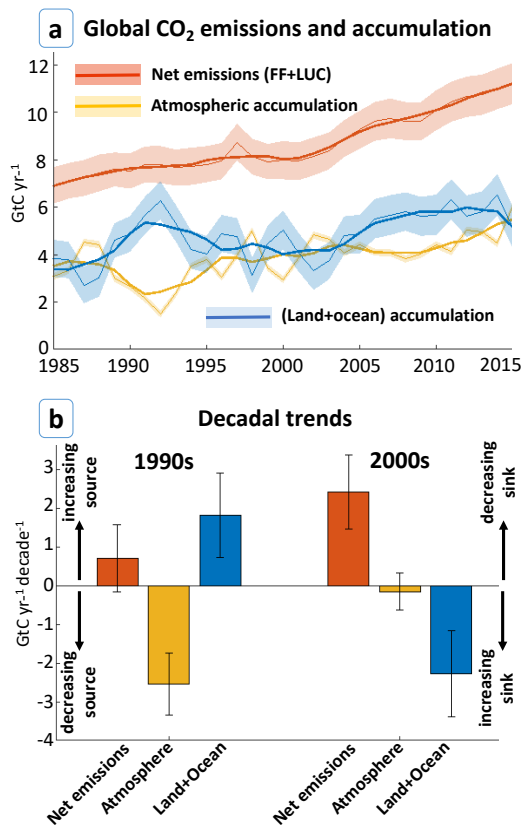


Fig. 1. (a) Global CO₂ emissions from fossil-fuel burning, cement production and land-use change (FF+LUC) (red curve), compared with the measured rate of accumulation of CO₂ in the atmosphere (gold curve), and the inferred rate of change of CO₂ accumulation in the land and ocean (blue curve). Thin lines are annual means and thick lines are 5-year running means. (b) Decadal trends in CO₂ emissions (FF+LUC), and the atmospheric and total land+ocean sinks. For emissions, positive values indicate an increasing source and negative values a decreasing source (left-hand arrows, opposite the sign convention as in Eq. (1)). For the atmosphere and land+ocean sinks, positive values indicate a decreasing sink and negative values an increasing sink (right-hand arrows, opposite the sign convention in Eq. (1)). All data from the 2017 Global Carbon Budget (3). Error bars are 1- σ .

estimating CO₂ accumulation in the ocean indirectly from observations using inverse models (9–11), and measurements of the sea-surface partial pressure of CO₂ (pCO₂) (12–14).

While the terrestrial biosphere is the dominant source of interannual variability in the natural CO₂ sinks (4, 15), observations and numerical models have highlighted substantial decadal variability in ocean CO₂ uptake at both regional (16–18) and global scales (19, 20). In particular, recent estimates from several data-based models (21–23) suggest that the decadal variability in the ocean CO₂ sink is larger than currently estimated by global carbon budgets. To assess the robustness of decadal trends in ocean CO₂ uptake, here we compare decadal variability in the ocean carbon sink from three widely-used independent methods: GOBMs participating in the 2017 Global Carbon Budget (3), an ocean circulation inverse model (OCIM) (11, 23), and pCO₂-based flux mapping models from the Surface Ocean pCO₂ Mapping Intercomparison (SOCOM) project (14). We use these methods to deduce the contribution of the ocean carbon sink to the decadal variability of atmospheric carbon accumulation, to examine the mechanisms governing this variability, and to shed light on the decadal variability of the terrestrial CO₂ sink.

Decadal variability of the ocean carbon sink

Estimates of the global ocean carbon sink from the GOBMs, SOCOM products, and the OCIM are in broad agreement regarding the magnitude and temporal evolution of ocean carbon accumulation over the past 30 years (Fig. 2a). Estimates of the ocean anthropogenic carbon sink in 2010 from these methods cluster around a mean of ~ 2.4 GtC yr⁻¹ with an uncertainty of $\sim 25\%$ due to differences among the various methods and models (Fig. 2a).

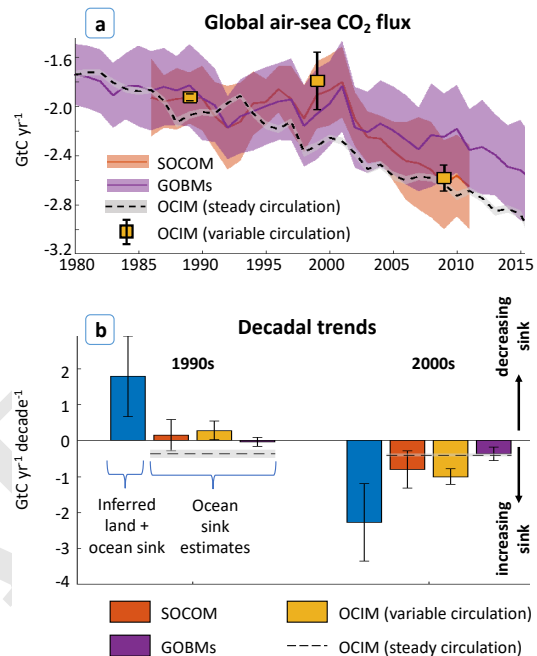


Fig. 2. (a) Estimates of the ocean carbon sink from a subset of models participating in the Surface Ocean pCO₂ Mapping (SOCOM) project (14), a subset of Global Ocean Biogeochemical Models (GOBMs) participating in the 2017 Global Carbon Budget (3) and an ocean circulation inverse model (OCIM) with (23) and without (11) decadal variability in ocean circulation. Thick lines are the ensemble mean from each method, with shading representing one standard deviation uncertainty. For the OCIM with variable circulation the mean value at the end of each decade (1989, 1999, 2009) is shown, with error bars representing one standard deviation. For the OCIM with constant circulation, error bars are the ensemble range. SOCOM results have been adjusted for outgassing of riverine CO₂ (see Materials and Methods). (b) Decadal trends in the net (land+ocean) carbon sink (blue bar, same as in Fig. 1), and four estimates of decadal trends in the ocean carbon sink from SOCOM models (red bar), GOBMs (purple bar), and OCIM with decadal variability in ocean circulation (gold bar) and without any variability in ocean circulation (dashed line).

A closer look at the decadal trends in ocean CO₂ uptake reveals that the various methods of estimating the oceanic CO₂ sink differ in the magnitude of their decadal variability (Fig. 2b). The OCIM with steady circulation simulates CO₂ uptake by an ocean with no variability in circulation or biology (11), and therefore the decadal trends are very similar for both the 1990s and the 2000s, with global ocean CO₂ accumulation accelerating at ~ 0.4 Gt C yr⁻¹ decade⁻¹. All of the other methods display significantly more decadal variability, strongly suggesting decadal trends in ocean circulation and/or biology over this time period (Fig. 2b).

Decadal trends in ocean CO₂ uptake are strongest in the observation-based models. In the 1990s, SOCOM products (14) and the OCIM with decadal variability in ocean circulation (23)

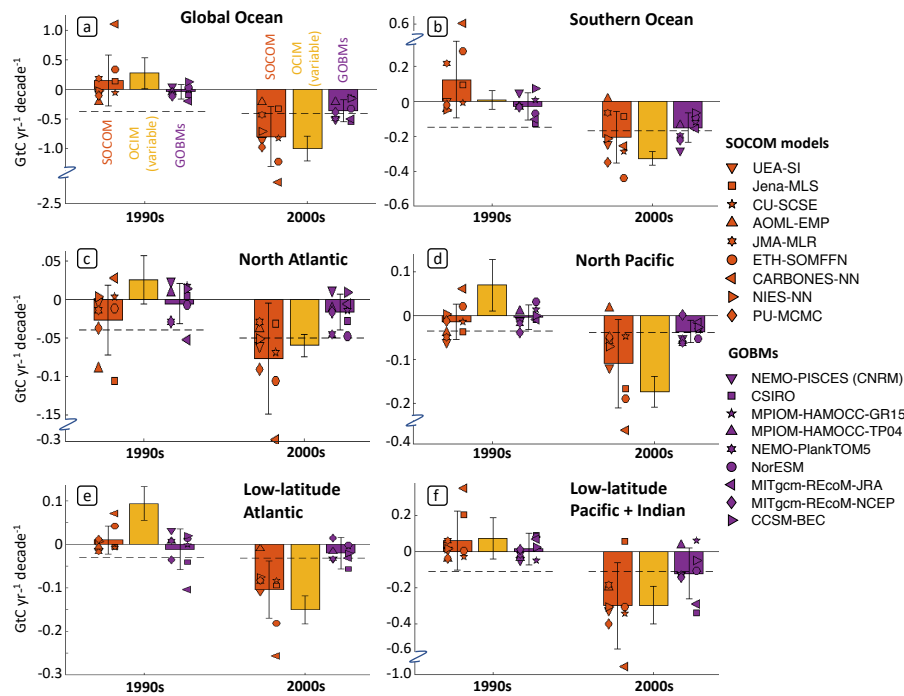


Fig. 3. Decadal trends in ocean carbon uptake for the global ocean (a) and for different ocean regions (b-f) as defined by the biomes of (24) (see SI Appendix for biome definitions, and definitions of the models used here). The global ocean in (a) is the sum of the regions in (b-f) and does not include coastal regions and marginal seas. Trends and color-coding as in Fig. 2(b), with symbols representing individual models. Positive trends represent a weakening oceanic CO₂ sink, and negative trends a strengthening oceanic CO₂ sink.

95 diagnose a weakening trend of $0.15 \pm 0.43 \text{ Gt C yr}^{-1} \text{ decade}^{-1}$ and $0.28 \pm 0.26 \text{ Gt C yr}^{-1} \text{ decade}^{-1}$, respectively, which
 96 in turn accounts for 8% ($-10 - 83\%$) and 16% ($1 - 77\%$) of
 97 the observed $1.8 \pm 1.1 \text{ Gt C yr}^{-1} \text{ decade}^{-1}$ weakening of the
 98 net (land+ocean) carbon sink. In the 2000s, the SOCOM
 99 products estimate a strengthening of the ocean carbon sink
 100 by $0.80 \pm 0.51 \text{ Gt C yr}^{-1} \text{ decade}^{-1}$ that is consistent with the
 101 $1.0 \pm 0.2 \text{ Gt C yr}^{-1} \text{ decade}^{-1}$ strengthening inferred by the
 102 OCIM with variable circulation. These trends account for 35%
 103 ($9 - 109\%$) and 43% ($24 - 100\%$), respectively, of the observed
 104 $2.3 \pm 1.1 \text{ Gt C yr}^{-1} \text{ decade}^{-1}$ strengthening trend of the total
 105 (land+ocean) carbon sink in the 2000s. Based on the average
 106 trends in the observation-based models over the 1990s and
 107 the first decade of the 2000s, the ocean is responsible for $\sim 10\text{-}40\%$
 108 of the observed decadal variability in the natural carbon sinks.
 109

110 The GOBMs also simulate weaker-than-expected ocean
 111 CO₂ uptake during the 1990s followed by a strengthening trend
 112 during the 2000s, but the magnitude of decadal variability
 113 is smaller than that estimated by SOCOM and the variable-
 114 circulation OCIM. For example, in the 2000s the growth rate
 115 of oceanic CO₂ uptake in the GOBMs was slightly less than
 116 simulated by the OCIM with constant circulation and biology,
 117 while the other methods estimate that oceanic uptake was
 118 accelerating roughly twice as fast as it would with constant
 119 circulation and biology (Fig. 2b). According to average
 120 trends in the GOBMs over 1990s and the first decade of the
 121 2000s, the ocean is responsible for $\sim 0\text{-}20\%$ of the decadal
 122 variability in the natural carbon sinks, which is about half of
 123 the variability estimated by the observation-based approaches.
 124

125 Despite the overall agreement among the methods on the
 126 sign of the decadal variability in the ocean CO₂ sink, there

126 is substantial spread in the magnitude of the decadal trends
 127 both across models within a particular method, and across
 128 oceanographic regions (Fig. 3). With respect to the global
 129 ocean CO₂ uptake, the SOCOM products range from a trend of
 130 -0.21 to $1.11 \text{ Gt C yr}^{-1} \text{ decade}^{-1}$ in the 1990s, to -0.21 to -2.13
 131 $\text{Gt C yr}^{-1} \text{ decade}^{-1}$ in the 2000s. Almost all (eight out of nine)
 132 of the SOCOM products show a more rapidly strengthening
 133 CO₂ sink in the 2000s compared to the 1990s. Different
 134 GOBMs also exhibit substantially different decadal variability,
 135 although all of the GOBMs simulate a strengthening of the
 136 ocean CO₂ sink in the 2000s relative to the 1990s (Fig. 3a).

137 To examine regional patterns of decadal variability in the
 138 ocean CO₂ sink, we integrated the air-sea CO₂ fluxes within
 139 different regions based on biomes defined by ref. (24) (see SI
 140 Appendix). The model-average trends across different methods
 141 (SOCOM, GOBMs, and OCIM), and in different oceanographic
 142 regions, display a remarkable pattern: in every region every
 143 method (on average) predicts that the oceanic CO₂ uptake
 144 increased faster in the 2000s than in the 1990s (Fig. 3b-f).
 145 The best agreement at regional scales across methods is found
 146 between the SOCOM products and the OCIM with variable
 147 circulation. In all regions these methods infer an oceanic CO₂
 148 sink that strengthened much faster in the 2000s than in the
 149 1990s. In the high latitudes, the SOCOM-based estimates
 150 place more of the weakening in the 1990s CO₂ sink in the
 151 Southern Ocean, while the OCIM-based estimates suggest that
 152 more of the weakening occurred in the North Atlantic and
 153 North Pacific (Fig. 3b-d). In the low-latitudes, the SOCOM
 154 and OCIM models agree that the Pacific and Indian Oceans
 155 were a weakening sink in the 1990s (Fig. 3f), while the OCIM
 156 simulates a weaker-trending Atlantic Ocean sink than most of

157 the SOCOM products (Fig. 3e). The strengthening of the
 158 ocean CO₂ sink in the 2000s is consistent across regions in
 159 both the SOCOM and OCIM models.

160 Decadal trends in the GOBM-simulated oceanic CO₂ up-
 161 take are not as variable as those diagnosed by the SOCOM
 162 products or the variable-circulation OCIM. For example, in
 163 the Southern Ocean the observation-based methods infer large
 164 decadal variations in the ocean CO₂ sink, but the GOBMs
 165 simulate only a slight strengthening trend from the 1990s to
 166 the 2000s, with the exception of the NEMO-PISCES (CNRM)
 167 model which simulates a large strengthening (Fig. 3b). The
 168 same is true in the low-latitude Pacific and Indian, which has
 169 the largest decadal variability next to the Southern Ocean in
 170 the observation-based estimates, but displays weak decadal
 171 variability in the GOBMs (Fig. 3f).

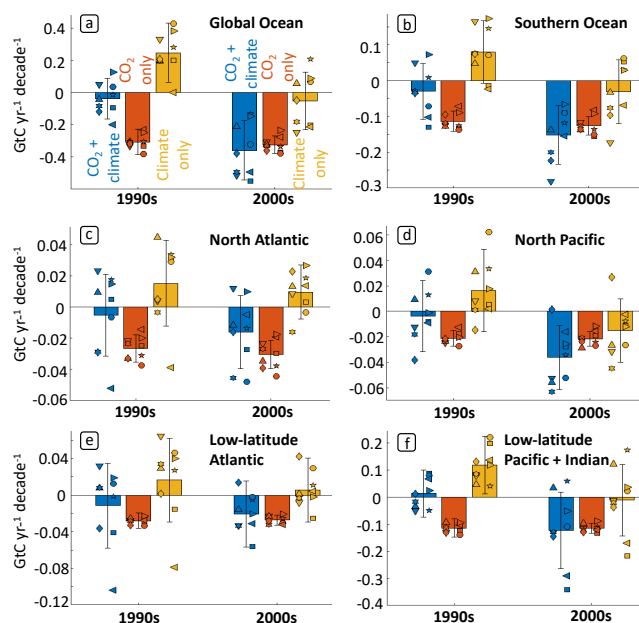
172 Climate-driven trends in ocean carbon uptake

173 To separate the impacts of CO₂-forced and climate-forced
 174 variability on ocean CO₂ uptake in the GOBMs, we performed
 175 additional model simulations in which the climate forcing was
 176 held constant, and in which the atmospheric CO₂ concentra-
 177 tion was held constant (see Materials and Methods). Based
 178 on these simulations we isolated the decadal trends of oceanic
 179 CO₂ uptake due to atmospheric CO₂ increase and due to
 180 climate variability (Fig. 4). These simulations reveal that
 181 trends in ocean CO₂ uptake in the 1990s and 2000s are nearly
 182 indistinguishable for the CO₂-only forcing case (both between
 183 decades and among models), and that decadal variability in
 184 the CO₂ sink is driven exclusively by climate variability. Eight
 185 out of nine of the GOBMs predict that climate variability
 186 drove a weakening of the global ocean CO₂ sink in the 1990s,
 187 and five out of nine predict that climate variability drove a
 188 strengthening trend in the 2000s (Fig. 4a).

189 The regions with the strongest climate-driven decadal vari-
 190 ability in the GOBMs are the Southern Ocean (Fig 4b) and
 191 the low-latitude Pacific and Indian Oceans (Fig 4f). Within
 192 these regions, however, the different models diverge substan-
 193 tially. In the Southern Ocean the NEMO-PISCES (CNRM)
 194 model displays the largest climate-driven decadal variability,
 195 with decreasing CO₂ uptake in the 1990s and increasing CO₂
 196 uptake in the 2000s, consistent with the observation-based
 197 estimates. But some models display the opposite trend, such
 198 as the CSIRO model which simulates a weakening Southern
 199 Ocean CO₂ sink in the 2000s compared to the 1990s. In
 200 the low-latitude Pacific and Indian Oceans it is the CSIRO
 201 model that displays the strongest climate-driven variability, in
 202 a direction consistent with the observation-based estimates.

203 Overall, climate variability drove a weakening of oceanic
 204 CO₂ uptake in the 1990s and a strengthening in the 2000s
 205 across multiple models and geographic regions. The geograph-
 206 ical consistency of these trends suggests that this is a response
 207 to a global climatic pattern, likely large-scale changes in wind-
 208 driven ocean circulation (23, 25). These trends could be due to
 209 modes of internal variability in the climate system (21), or to
 210 external forcing (e.g. the eruption of Mount Pinatubo in 1991
 211 (26, 27)) which can alter the states of internal climate modes
 212 (28), and thus the global winds. External drivers could be
 213 amplified by atmospheric (29) or oceanic (30) teleconnections
 214 to enhance decadal variability in ocean circulation.

215 Although the GOBMs display a consistent response to cli-
 216 mate forcing, their climate-driven variability of ocean CO₂



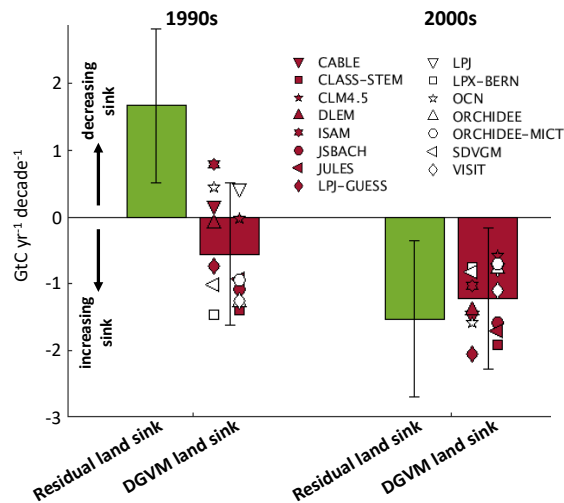
217
218
219
220
221
222
223
224
225
226
227
228
229
230
231
232
233
234
235
236
237
238
239
240
241
242
243
244
245
246
247
248
249
250
251
252
253
254
255
256
257
258
259
260
261
262
263
264
265
266
267
268
269
270
271
272
273
274
275
276
277
278
279
280
281
282
283
284
285
286
287
288
289
290
291
292
293
294
295
296
297
298
299
300
301
302
303
304
305
306
307
308
309
310
311
312
313
314
315
316
317
318
319
320
321
322
323
324
325
326
327
328
329
330
331
332
333
334
335
336
337
338
339
340
341
342
343
344
345
346
347
348
349
350
351
352
353
354
355
356
357
358
359
360
361
362
363
364
365
366
367
368
369
370
371
372
373
374
375
376
377
378
379
380
381
382
383
384
385
386
387
388
389
390
391
392
393
394
395
396
397
398
399
400
401
402
403
404
405
406
407
408
409
410
411
412
413
414
415
416
417
418
419
420
421
422
423
424
425
426
427
428
429
430
431
432
433
434
435
436
437
438
439
440
441
442
443
444
445
446
447
448
449
450
451
452
453
454
455
456
457
458
459
460
461
462
463
464
465
466
467
468
469
470
471
472
473
474
475
476
477
478
479
480
481
482
483
484
485
486
487
488
489
490
491
492
493
494
495
496
497
498
499
500
501
502
503
504
505
506
507
508
509
510
511
512
513
514
515
516
517
518
519
520
521
522
523
524
525
526
527
528
529
530
531
532
533
534
535
536
537
538
539
540
541
542
543
544
545
546
547
548
549
550
551
552
553
554
555
556
557
558
559
560
561
562
563
564
565
566
567
568
569
570
571
572
573
574
575
576
577
578
579
580
581
582
583
584
585
586
587
588
589
590
591
592
593
594
595
596
597
598
599
600
601
602
603
604
605
606
607
608
609
610
611
612
613
614
615
616
617
618
619
620
621
622
623
624
625
626
627
628
629
630
631
632
633
634
635
636
637
638
639
640
641
642
643
644
645
646
647
648
649
650
651
652
653
654
655
656
657
658
659
660
661
662
663
664
665
666
667
668
669
670
671
672
673
674
675
676
677
678
679
680
681
682
683
684
685
686
687
688
689
690
691
692
693
694
695
696
697
698
699
700
701
702
703
704
705
706
707
708
709
710
711
712
713
714
715
716
717
718
719
720
721
722
723
724
725
726
727
728
729
730
731
732
733
734
735
736
737
738
739
740
741
742
743
744
745
746
747
748
749
750
751
752
753
754
755
756
757
758
759
760
761
762
763
764
765
766
767
768
769
770
771
772
773
774
775
776
777
778
779
780
781
782
783
784
785
786
787
788
789
790
791
792
793
794
795
796
797
798
799
800
801
802
803
804
805
806
807
808
809
810
811
812
813
814
815
816
817
818
819
820
821
822
823
824
825
826
827
828
829
830
831
832
833
834
835
836
837
838
839
840
841
842
843
844
845
846
847
848
849
850
851
852
853
854
855
856
857
858
859
860
861
862
863
864
865
866
867
868
869
870
871
872
873
874
875
876
877
878
879
880
881
882
883
884
885
886
887
888
889
890
891
892
893
894
895
896
897
898
899
900
901
902
903
904
905
906
907
908
909
910
911
912
913
914
915
916
917
918
919
920
921
922
923
924
925
926
927
928
929
930
931
932
933
934
935
936
937
938
939
940
941
942
943
944
945
946
947
948
949
950
951
952
953
954
955
956
957
958
959
960
961
962
963
964
965
966
967
968
969
970
971
972
973
974
975
976
977
978
979
980
981
982
983
984
985
986
987
988
989
990
991
992
993
994
995
996
997
998
999
1000

uptake appears to be too weak when compared to the data-
 based methods. Indeed, the GOBMs that perform best when
 compared to the most accurate pCO₂-based flux reconstruc-
 tions, are also the models that exhibit the largest decadal
 variability at the regional scale (SI Appendix Figs. S1 and
 S2). The weak climate-forced variability of GOBMs might
 stem from either a weak ocean circulation response to atmo-
 spheric forcing, or to changes in biologically-driven carbon
 uptake that counteract circulation-driven CO₂ uptake. To
 examine the latter possibility, we examined decadal trends
 in the biologically-driven export of carbon below the surface
 ocean in the climate-forced GOBMs (SI Appendix Fig. S3).
 Models with strong decadal variability in biological carbon
 export generally have weak decadal variability in climate-
 forced CO₂ uptake, while the opposite is true of models
 with weak decadal variability in biological carbon export.
 Thus the compensation between circulation-driven and bio-
 logically-driven CO₂ uptake is one factor that reduces the
 sensitivity of the GOBMs to climate variability. The relative
 roles of biology and physics for determining decadal vari-
 ability in ocean CO₂ uptake is poorly known, and should
 be a priority for future study.

Discussion and conclusions

The agreement among the various methods of determining
 ocean CO₂ uptake demonstrates a broad consensus in the
 magnitude of the ocean carbon sink over the past several
 decades, and in the timing of the decadal variability (Fig.
 2). This agreement is especially encouraging considering that
 the three methods considered here are entirely independent.
 The observation-based methods (SOCOM and OCIM) predict
 greater decadal variability of the ocean CO₂ sink than ocean

247 biogeochemistry models, and suggest that roughly 10-40% of
 248 the decadal variability in the natural CO₂ sinks can be at-
 249 tributed to the ocean. Ocean biogeochemistry models simulate
 250 less decadal variability of the ocean CO₂ sink, which could
 251 partly explain why current global carbon budgets (which rely
 252 mainly on GOBMs to estimate the oceanic CO₂ sink) have
 253 a declining budget imbalance in the 1990s, followed by an
 254 increasing imbalance in the 2000s (3). A muted variability of
 255 GOBMs compared to observations has also been observed for
 256 oxygen (31), suggesting it is not unique to the carbon cycle.
 257 These results also have important implications for decadal
 258 trends in the other major natural sink of anthropogenic CO₂,
 259 the terrestrial biosphere. The decadal trends in the ocean CO₂
 260 sink from the three methods considered here (SOCOM, OCIM,
 261 and GOBMs), can be compared to the total land+ocean CO₂
 262 sink (Fig. 1b), to deduce the decadal trends in the terrestrial
 263 CO₂ sink (see Materials and Methods). The decadal trends in
 264 the terrestrial CO₂ sink so calculated demonstrate that the
 265 terrestrial biosphere was a decreasing sink of CO₂ in the 1990s,
 266 and an increasing sink of CO₂ in the first decade of the 2000s
 267 (the residual land sink in Fig. 5).



268 **Fig. 5.** Trends in the terrestrial CO₂ sink calculated as a residual from the global
 269 carbon budget (Equation 1) using the estimates of the ocean CO₂ sink from three
 270 methods considered here (GOBMs, SOCOM, and OCIM with variable circulation),
 271 and from the dynamic global vegetation models (DGVMs) participating in the 2017
 272 Global Carbon Budget (3). See SI Appendix for definitions of DGVMs used here.

268 These decadal trends are in the same direction as those of
 269 the oceanic CO₂ sink, but even larger in magnitude, and can
 270 place important constraints on the dynamic global vegetation
 271 models (DGVMs) that are used to estimate the terrestrial
 272 CO₂ sink in the Global Carbon Budget (3). The DGVMs
 273 are in good agreement with the residual land sink regarding
 274 the strengthening of the terrestrial CO₂ sink in the 2000s,
 275 indicating consistency between the emissions data, the ocean
 276 CO₂ sink estimates, and the predictions of DGVMs during this
 277 period (Fig. 5). But during the 1990s, the DGVMs show less
 278 consistency, with one group of DGVMs simulating a neutral
 279 to weakening CO₂ sink (in agreement with the residual land
 280 sink), and another group simulating a strengthening CO₂ sink.
 281 Differences between the residual land sink and the DGVM
 282 land sink during the 1990s could be due to biases in the ocean
 283 CO₂ sink estimates, in the CO₂ emissions, or in the DGVMs.
 284 Given the agreement between the three independent estimates

285 of the oceanic CO₂ sink, this is unlikely to be a source of bias.
 286 Errors in fossil-fuel CO₂ emissions (32) and LUC emissions
 287 (33) could be larger than reported, and partly responsible for
 288 some of the discrepancy. The remaining discrepancies can be
 289 attributed to biases in the DGVMs, and as such could indicate
 290 a greater climate sensitivity of the terrestrial CO₂ sink than
 291 currently thought. In particular, the model discrepancies in the
 292 1990s trends could partly reflect the different degrees to which
 293 the DGVMs are sensitive to the eruption of Mt. Pinatubo in
 294 1991 (34) and the strong El Niño event of 1998 (15).

295 The findings of this study imply that both oceanic and
 296 terrestrial carbon cycle models underestimate decadal variability
 297 in CO₂ uptake, which hinders the ability of these models
 298 to predict climate change on decadal timescales, and likely
 299 contributes to decadal imbalances in current global carbon
 300 budgets (35). As the community moves towards decadal climate
 301 prediction (36, 37), it will be important to correctly
 302 resolve the climate sensitivity of oceanic and terrestrial carbon
 303 uptake. Continued development of observation-based methods
 304 for tracking ocean CO₂ uptake should alleviate their remain-
 305 ing structural errors (see SI Appendix), leading to improved
 306 constraints on the magnitude and variability of the ocean CO₂
 307 sink, and reducing imbalances in global carbon budgets (35).
 308 This in turn will facilitate calibration of ocean biogeochemical
 309 models and terrestrial dynamic vegetation models, leading to
 310 improved climate projections and decadal predictions.

311 Materials and Methods

312 **pCO₂-based flux mapping products.** The surface ocean pCO₂ map-
 313 ping (SOCOM) products are based on historical observations of
 314 surface-ocean pCO₂ compiled in the Surface Ocean CO₂ Atlas
 315 (SOCAT) (38) and the Lamont-Doherty Earth Observatory (39)
 316 datasets. The SOCOM models employ various interpolation schemes
 317 to fill in the gaps in the data records to create continuous maps of
 318 pCO₂ at monthly resolution, from which air-sea fluxes are calculated
 319 (14). See SI Appendix for additional information.

320 **Inverse models.** We used two versions of the ocean circulation inverse
 321 model (OCIM). The first diagnoses the uptake of anthropogenic
 322 CO₂ in the absence of any changes to ocean circulation, solubility,
 323 or biology (11). Uncertainties are derived from the 10 different
 324 versions of the model described in ref. (11). The second version of
 325 the OCIM diagnoses the decadal-mean ocean CO₂ sink given decadal
 326 variations in ocean circulation along with mean state biology (23).
 327 Uncertainties are derived from 160 different versions of the model
 328 described in ref. (23). See SI Appendix for additional information.

329 **Global ocean biogeochemistry models (GOBMs).** We used a sub-
 330 set of the global ocean biogeochemistry models (GOBMs) used
 331 in the 2017 Global Carbon Budget (GCB17) (3): NEMO-
 332 PISCES (CNRM), CSIRO, NorESM, MPIOM-HAMOC, NEMO-
 333 PlankTOM5, MITgcm-REcoM2, and CCSM-BEC. Each model
 334 performed three simulations: Simulation A uses reanalysis climate
 335 forcing and observed atmospheric CO₂ concentrations 1959-2017.
 336 Simulation B uses constant climate forcing and atmospheric CO₂.
 337 Simulation C uses constant climate forcing and observed atmo-
 338 spheric CO₂ concentrations 1959-2017. In Figure 4, “CO₂+climate”
 339 is from simulation A, “CO₂ only” is from simulation C— simulation
 340 B, and “climate only” is from simulation A – simulation C. Models
 341 differ in their spin-up procedure and climate forcing, as detailed in
 342 the SI Appendix and Table S1.

343 **Accounting for riverine carbon.** The OCIM and GOBMs do not ac-
 344 count for a de-gassing of 0.45-0.78 GtC yr⁻¹ (40, 41) of riverine
 345 CO₂, but the SOCOM products do. In order to make the CO₂
 346 fluxes comparable across all methods, we have added a flux of 0.6
 347 GtC yr⁻¹ to the globally-integrated SOCOM CO₂ sink in Fig. 2.
 348

349 **Calculating decadal trends.** Air-sea CO₂ fluxes from the SOCOM
 350 products, the GOBMs, and the steady-circulation OCIM were
 351 annually-averaged, then used to compute the linear trend in ocean
 352 CO₂ uptake for the 1990s (1990-1999) and the first decade of the
 353 2000s (2000-2009). Uncertainties on the decadal trends for each
 354 method include ensemble uncertainty, as well as an uncertainty
 355 of ±1 year for the beginning and ending years of the trend calcu-
 356 lations (i.e. 1990 ± 1 – 1999 ± 1 and 2000 ± 1 – 2009 ± 1). For
 357 the OCIM-variable, decadal trends were calculated as the average
 358 air-sea flux within a given decade minus the average air-sea flux in
 359 the preceding decade. This method minimizes the effects of disconti-
 360 nuities in the air-sea CO₂ flux introduced by abrupt changes in the
 361 ocean circulation at the demarcations of different decades (1990 and
 362 2000), and gives trends similar to those using the final year of each
 363 decade (i.e. 2009-1999) to calculate trends. For regional decadal
 364 trends in Figs. 3 and 4, we integrated the air-sea CO₂ fluxes over
 365 distinct oceanographic regions based on the time-mean open-ocean
 366 biomes defined by ref. (24). In order to avoid differences in the
 367 model domains near the coast, the global ocean CO₂ uptake in all
 368 figures is the summation over all of the individual regions, and thus
 369 ignores a small contribution from coastal regions as well as the polar
 370 ice-covered regions. See SI Appendix for more information.

371 **Calculation of decadal trends in the terrestrial CO₂ sink.** To calcu-
 372 late decadal trends in the terrestrial CO₂ sink, we first calculated
 373 decadal trends in the ocean carbon sink using all of the methods con-
 374 sidered here that resolve decadal variability in the ocean CO₂ sink
 375 (SOCOM, GOBMs, and OCIM-variable, as displayed in Fig. 2b).
 376 We then subtracted these ocean-only trends from the trend in the
 377 total (land+ocean) CO₂ sink (Fig. 1b) to obtain the trends in
 378 the “residual land sink” (Fig. 5). Reported uncertainties include
 379 uncertainty in the CO₂ emissions, uncertainty in the atmospheric
 380 CO₂ concentration, uncertainty in the ocean CO₂ sink (treating
 381 all methods of estimating the ocean CO₂ sink as equally probable),
 382 and uncertainty due to varying the beginning and ending years for
 383 the trend calculation by ±1 year. Trends in the terrestrial CO₂ sink
 384 in the DGVMs are calculated in exactly the same way as those for
 385 the GOBMs, varying the starting and ending points of the trend
 386 calculation for each DGVM by ± 1 year. See SI Appendix for a full
 387 list of the DGVMs used here.

388 **Data availability.** OCIM data are available from the lead author and
 389 at <https://devries.eri.ucsb.edu/models-and-data-products/>. Timeseries
 390 of the SOCOM data following ref. (14) can be obtained from
 391 <http://www.bgc-jena.mpg.de/SOCOM/>. Timeseries of the GOBM data
 392 are available at (url to follow upon acceptance).

393 **ACKNOWLEDGMENTS.** We thank Rebecca Wright and Erik
 394 Buitenhuis at University of East Anglia, Norwich, for providing
 395 updated runs from the NEMO-PlankTOM5 model. TD acknowl-
 396 edges support from NSF grant OCE-1658392. CL thanks the UK
 397 Natural Environment Research Council for funding to the SONATA
 398 project (no. NE/P021417/1). PL was supported by the Max Planck
 399 Society for the Advancement of Science. JH was supported under
 400 Helmholtz Young Investigator Group Marine Carbon and Ecosystem
 401 Feedbacks in the Earth System (MarESys), grant number
 402 VH-NG-1301. SB and RS thank the H2020 project CRESCENDO
 403 “Coordinated Research in Earth Systems and Climate: Experiments,
 404 kNowledge, Dissemination and Outreach” which received funding
 405 from the European Union’s Horizon 2020 research and innovation
 406 program under grant agreement No 641816. The Surface Ocean
 407 CO₂ Atlas (SOCAT) is an international effort, endorsed by the
 408 International Ocean Carbon Coordination Project (IOCCP), the
 409 Surface Ocean-Lower Atmosphere Study (SOLAS) and the Inte-
 410 grated Marine Biosphere Research (IMBeR) program, to deliver
 411 a uniformly quality-controlled surface ocean CO₂ database. The
 412 many researchers and funding agencies responsible for the collection
 413 of data and quality control are thanked for their contributions to
 414 SOCAT.

415 1. Myhre G, et al. (2013) *Anthropogenic and Natural Radiative Forcing*, eds. Stocker T, et al.
 416 (Cambridge University Press, Cambridge, United Kingdom and New York, NY, USA), p.
 417 659–740.
 418 2. Ciais P, et al. (2013) *Carbon and Other Biogeochemical Cycles*, eds. Stocker T, et al. (Cam-
 419 bridge University Press, Cambridge, United Kingdom and New York, NY, USA), p. 465–570.

420 3. Le Quéré C, et al. (2018) Global carbon budget 2017. *Earth System Science Data* 10(1):405–
 421 448.
 422 4. Keenan TF, et al. (2016) Recent pause in the growth rate of atmospheric co₂ due to enhanced
 423 terrestrial carbon uptake. *Nature communications* 7:13428.
 424 5. Burton MR, Sawyer GM, Granieri D (2013) Deep carbon emissions from volcanoes. *Reviews*
 425 *in Mineralogy and Geochemistry* 75(1):323–354.
 426 6. Andres RJ, Boden TA, Higon D (2014) A new evaluation of the uncertainty associated with
 427 cdia estimates of fossil fuel carbon dioxide emission. *Tellus B: Chemical and Physical Mete-*
 428 *orology* 66(1):23616.
 429 7. Ballantyne A, et al. (2015) Audit of the global carbon budget: estimate errors and their impact
 430 on uptake uncertainty. *Biogeosciences (Online)* 12(8).
 431 8. Conway TJ, et al. (1994) Evidence for interannual variability of the carbon cycle from the
 432 national oceanic and atmospheric administration/climate monitoring and diagnostics labo-
 433 ratory global air sampling network. *Journal of Geophysical Research: Atmospheres*
 434 99(D11):22831–22855.
 435 9. Gruber N, et al. (2009) Oceanic sources, sinks, and transport of atmospheric co₂. *Global*
 436 *Biogeochemical Cycles* 23(1).
 437 10. Khatiwala S, Primeau F, Hall T (2009) Reconstruction of the history of anthropogenic co₂
 438 concentrations in the ocean. *Nature* 462(7271):346.
 439 11. DeVries T (2014) The oceanic anthropogenic co₂ sink: Storage, air-sea fluxes, and trans-
 440 ports over the industrial era. *Global Biogeochemical Cycles* 28(7):631–647.
 441 12. Takahashi T, et al. (2009) Climatological mean and decadal change in surface ocean pco₂,
 442 and net sea–air co₂ flux over the global oceans. *Deep Sea Research Part II: Topical Studies*
 443 *in Oceanography* 56(8-10):554–577.
 444 13. Landschützer P, Gruber N, Bakker D, Schuster U (2014) Recent variability of the global ocean
 445 carbon sink. *Global Biogeochemical Cycles* 28(9):927–949.
 446 14. Rödenbeck C, et al. (2015) Data-based estimates of the ocean carbon sink variability—first re-
 447 sults of the surface ocean pco₂ mapping intercomparison (socom). *Biogeosciences* 12:7251–
 448 7278.
 449 15. Kim JS, Kug JS, Yoon JH, Jeong SJ (2016) Increased atmospheric co₂ growth rate dur-
 450 ing el niño driven by reduced terrestrial productivity in the cmp5 esms. *Journal of Climate*
 451 29(24):8783–8805.
 452 16. Takahashi T, Sutherland SC, Feely RA, Cosca CE (2003) Decadal variation of the surface
 453 water pco₂ in the western and central equatorial pacific. *Science* 302(5646):852–856.
 454 17. Landschützer P, et al. (2015) The reinvigoration of the southern ocean carbon sink. *Science*
 455 349(6253):1221–1224.
 456 18. Breeden ML, McKinley GA (2016) Climate impacts on multidecadal pco₂ variability in the
 457 north atlantic: 1948–2009. *Biogeosciences* 13(11):3387–3396.
 458 19. Fay A, McKinley G (2013) Global trends in surface ocean pco₂ from in situ data. *Global*
 459 *Biogeochemical Cycles* 27(2):541–557.
 460 20. Séférian R, Berthet S, Chevallier M (2018) Assessing the decadal predictability of land and
 461 ocean carbon uptake. *Geophysical Research Letters* 45(5):2455–2466.
 462 21. Landschuetzer P, Gruber N, Bakker DC (2016) Decadal variations and trends of the global
 463 ocean carbon sink. *Global Biogeochemical Cycles* 30(10):1396–1417.
 464 22. Landschützer P, Ilyina T, Lovenduski NS (2019) Detecting Regional Modes of Variability in
 465 Observation-Based Surface Ocean pCO₂. *Geophysical Research Letters*.
 466 23. DeVries T, Holzer M, Primeau F (2017) Recent increase in oceanic carbon uptake driven by
 467 weaker upper-ocean overturning. *Nature* 542(7640):215.
 468 24. Fay A, McKinley G (2014) Global open-ocean biomes: mean and temporal variability. *Earth*
 469 *System Science Data* 6(2):273–284.
 470 25. Le Quéré C, Takahashi T, Buitenhuis ET, Rödenbeck C, Sutherland SC (2010) Impact of
 471 climate change and variability on the global oceanic sink of co₂. *Global Biogeochemical*
 472 *Cycles* 24(4).
 473 26. Frölicher T, Joos F, Raible C (2011) Sensitivity of atmospheric co₂ and climate to explosive
 474 volcanic eruptions. *Biogeosciences* 8(8):2317–2339.
 475 27. Raupach MR, et al. (2014) The declining uptake rate of atmospheric co₂ by land and ocean
 476 sinks. *Biogeosciences* 11(13):3453–3475.
 477 28. Stevenson S, et al. (2018) Climate variability, volcanic forcing, and last millennium hydrocli-
 478 mate extremes. *Journal of Climate* 31(11):4309–4327.
 479 29. McGregor S, Stuecker MF, Kajtar JB, England MH, Collins M (2018) Model tropical atlantic
 480 biases underpin diminished pacific decadal variability. *Nature Climate Change* p. 1.
 481 30. Peterson RG, White WB (1998) Slow oceanic teleconnections linking the antarctic circum-
 482 polar wave with the tropical el niño-southern oscillation. *Journal of Geophysical Research:*
 483 *Oceans* 103(C11):24573–24583.
 484 31. Andrews O, Bindoff N, Halloran P, Ilyina T, Le Quéré C (2013) Detecting an external influence
 485 on recent changes in oceanic oxygen using an optimal fingerprinting method. *Biogeosciences*
 486 10:1799–1813.
 487 32. Saeki T, Patra P (2017) Implications of overestimated anthropogenic co₂ emissions on east
 488 asian and global land co₂ flux inversion. *Geoscience Letters* 4(9).
 489 33. Le Quéré C, et al. (2009) Trends in the sources and sinks of carbon dioxide. *Nature geo-*
 490 *science* 2(12):831.
 491 34. Frölicher TL, Joos F, Raible CC, Sarmiento JL (2013) Atmospheric co₂ response to vol-
 492 canic eruptions: The role of enso, season, and variability. *Global Biogeochemical Cycles*
 493 27(1):239–251.
 494 35. Quéré CL, et al. (2018) Global carbon budget 2018. *Earth System Science Data* 10(4):2141–
 495 2194.
 496 36. Boer GJ, et al. (2016) The decadal climate prediction project (dcpp) contribution to crip6.
 497 *Geoscientific Model Development* 9:3751–3777.
 498 37. Yeager S, et al. (2018) Predicting near-term changes in the earth system: A large ensemble
 499 of initialized decadal prediction simulations using the community earth system model. *Bulletin*
 500 *of the American Meteorological Society* pp. 1867–1886.
 501 38. Bakker DCE, et al. (2016) A multi-decade record of high-quality fco₂ data in version 3 of the
 502 surface ocean co₂ atlas (socat). *Earth System Science Data* 8(2):383–413.
 503 39. Takahashi T, Sutherland SC, Kozyr A (2014) Global ocean surface water partial pressure of

504 co2 database: Measurements performed during 1957-2013 (version 2013).
505 40. Jacobson AR, Mikaloff Fletcher SE, Gruber N, Sarmiento JL, Gloor M (2007) A joint
506 atmosphere-ocean inversion for surface fluxes of carbon dioxide: 1. methods and global-
507 scale fluxes. *Global Biogeochemical Cycles* 21(1).
508 41. Resplandy L, et al. (2018) Revision of global carbon fluxes based on a reassessment of
509 oceanic and riverine carbon transport. *Nature Geoscience* 11(7):504.

DRAFT